land

MDPI

Article

Ecological Network Construction Based on Ecosystem Services and Landscape Pattern Indices in the Tabu River Basin

Weichen Zhang, Yuyang Fan and Bojie Wang *

Collaborative Innovation Center for Grassland Ecological Security, School of Ecology and Environment, Inner Mongolia University, Hohhot 010021, China; 32215111@mail.imu.edu.cn (W.Z.); 32215178@mail.imu.edu.cn (Y.F.)

* Correspondence: wangbj@imu.edu.cn; Tel.: +86-185-8607-9228

Abstract: Unsustainable human activities threaten the ecological security of arid and semi-arid watersheds. However, improving the connectivity of ecological networks can enhance ecosystem services and preserve biodiversity in these fragile environments. In this study, we aimed to identify ecological sources of the Tabu River Basin by quantifying five key ecosystem services and using a morphological spatial pattern analysis model. We further optimized resistance surfaces using landscape pattern indices, constructed an ecological network, and provided recommendations for sustainable management. The results obtained were as follows: (1) Ecosystem services in the Tabu River Basin exhibit clear spatial heterogeneity, with significant increases in water yield, food supply, and carbon sequestration over the past two decades. (2) Landscape pattern indices, such as the aggregation index, patch cohesion index, and Shannon's diversity index, showed declines, indicating heightened landscape fragmentation and reduced connectivity. (3) Over the study period, the number of ecological sources increased from 6 to 17, although the total area of these sources decreased. The number of corridors expanded from 9 to 36, with a total length increase of 362.47 km, whereas pinch points increased from 27 to 40. (4) After optimization, one additional corridor and 24 new pinch points were identified, alongside a marked reduction in resistance in the northern and central-western regions. These results provide a robust scientific basis for optimizing land-use planning and reinforcing ecological security in the Tabu River Basin.

Keywords: ecosystem services; ecological network; landscape pattern indices; resistance surface optimization; biodiversity

check for updates

Citation: Zhang, W.; Fan, Y.; Wang, B. Ecological Network Construction Based on Ecosystem Services and Landscape Pattern Indices in the Tabu River Basin. *Land* **2024**, *13*, 2209. https://doi.org/10.3390/land13122209

Academic Editors: Qi Fu, Xu Bi, Kai Li and Hans Skov-Petersen

Received: 29 October 2024
Revised: 6 December 2024
Accepted: 14 December 2024
Published: 17 December 2024

Copyright: © 2024 by the authors. Licensee MDPI, Basel, Switzerland. This article is an open access article distributed under the terms and conditions of the Creative Commons Attribution (CC BY) license (https://creativecommons.org/licenses/by/4.0/).

1. Introduction

Rapid urbanization on a global scale has increasingly threatened ecological security and resulted in environmental issues [1,2]. In recent years, habitat loss and landscape fragmentation, with severe consequences on biodiversity and ecosystem services (ESs), have increased significantly in arid and semi-arid watersheds [3–5]. Ecological networks (ENs) highlight the dynamic balance within ecosystems and contribute to maintaining ecological security and protecting biodiversity [6]. ESs, which are the direct and indirect benefits that humans derive from ecosystems, provide essential resources that support human survival and wellbeing [7–9]. In ecologically vulnerable regions, such as arid and semi-arid regions, safeguarding and enhancing ESs is beneficial for the reasonable construction of ENs. Further, ecological corridors, which function as essential conduits for the flow of ecological energy, are crucial for linking ecological habitats, preserving biodiversity, and maintaining the stability of ENs via the proliferation of ESs [3,10].

The intricate landscape patterns of these corridors are also reflective of the overall ecological security of a given region. Landscape pattern indices also offer valuable insights into the structural composition, dynamic changes, and spatial distribution characteristics of ecological corridors [11]. The construction and optimization of ENs are of great significance

for ecological spatial management, regional sustainable development, and the overall stability of ecological function, which can contribute significantly to alleviating the problem of landscape fragmentation and biodiversity loss [6,12].

Considerable progress has been achieved in the construction of ENs over the past decade [13]. Notably, the construction of ENs includes the identification of ecological sources, the construction of ecological resistance surfaces, and the extraction of ecological corridors [14]. The use of morphological spatial pattern analysis (MSPA) has also become common in the identification of ecological sources and the scientific quantification of landscape morphology, structure, and pattern, thus improving the scientific basis and rationality for selecting ecosystem sources [1,6]. However, relative to ESs, this identification method does not comprehensively consider ecological processes. Therefore, MSPA, Ess, and landscape pattern indices have been applied to construct ecological sources with high ecological benefits and connectivity. Regarding the establishment of resistance surfaces, land-use types have been directly employed in many studies as a basis for resistance allocation [10]. However, this strategy is associated with a high degree of subjectivity; hence, it is prone to overlooking differences within the same land-use type in ecological resistance. Alternatively, researchers have incorporated area-specific indicators, such as nighttime population density and elevation, to refine resistance surfaces, thereby enabling a more accurate depiction of landscape variability [1].

Several methods, such as the gravity model, least-cost path (LCP) model, and minimum cumulative resistance (MCR) model, have been employed to identify and optimize ecological corridors [3]. Specifically, the MCR model, which emphasizes landscape unit connectivity via the "source-sink" approach while considering landscape heterogeneity and connectivity, is the most widely applied model [15,16]. Its usability can be attributed to the fact that it can comprehensively couples natural and human factors with low data demand and enables visualization of the results [6]. It also enables the identification of impediments to ecological flow from the source to the target destination and also simulates the process of ecological flow [17]. Therefore, we adopted the MCR model and Linkage Mapper, which are the basis for optimizing ecological corridors and ENs, to identify ecological pinch points and build ecological corridors and ENs [18].

Intermittent rivers constitute over 50% of the world's river network and are major contributors to water resource availability and biodiversity [19]. However, their importance has been frequently overlooked [20,21]. Further, these rivers, which stop flowing during certain periods and become limited within one or more reaches of the river network, are essential for providing ESs and ensuring human wellbeing [22]. The Tabu River Basin, which traverses arid and semi-arid zones, is intermittent. It is located in the agro-pastoral region of central Inner Mongolia and plays a central role in this region. It also holds a pivotal position at the heart of the northern windbreak and sand-fixing belt and functions as a crucial ecological security barrier with significant ecological implications. However, various human activities have had negative effects in recent years, such as urbanization and overgrazing, resulting in land degradation and habitat loss accompanied by significant issues of grassland desertification and soil salinization, which present a threat to ecological security [23].

In this study, we evaluated five ESs over a 20-year period and constructed ENs for the Tabu River Basin. The specific objectives were: (1) to analyze the changes and dynamics of ESs, including water yield (WY), habitat quality (HQ), food supply (FS), sand fixation (SF), and carbon sequestration (CS), from 2000 to 2020; (2) to identify the ecological core and calculate and optimize resistance surfaces using landscape pattern indices; and (3) to construct and optimize ecological corridors and ENs in the river basin for targeted management. The results of this study may facilitate the development of strategies that can be employed to ensure ecological security in the area we studied.

2. Methods

2.1. Study Area

The Tabu River Basin, which covers an area of approximately 3×10^4 km^2 is located in Inner Mongolia, China (41°2′–42°32′ N, 110°34′–112°11′ E). This river basin hosts the Tabu River, which is 322 km long, also known as the Xilamulun River, and is the largest inland river within the desert steppe region of the northern foothills of the Yin Mountains in terms of drainage area. The altitude of the basin ranges from 1009 to 2167 m, and the river flows through Siziwang Banner for the majority of its course. The terrain within the basin is complex and features high plains in the north and low mountainous hills in the south. The basin is also located deep in the hinterlands of the Eurasian continent and has a temperate continental climate. Its annual average temperature and precipitation are approximately 4 °C and less than 350 mm, respectively. In this basin, average annual evaporation is generally high and is approximately seven times the annual average precipitation. Further, with numerous tributaries, the basin relies mainly on precipitation for replenishment. Thus, the river in this basin is predominantly seasonal [24]. Furthermore, vegetation cover in this basin is dominated by desert steppes. Residential areas, artificial surfaces, and cultivated land are also densely distributed in the river-network south of the basin, whereas the north is covered by desert steppe and bare surfaces (Figure 1).

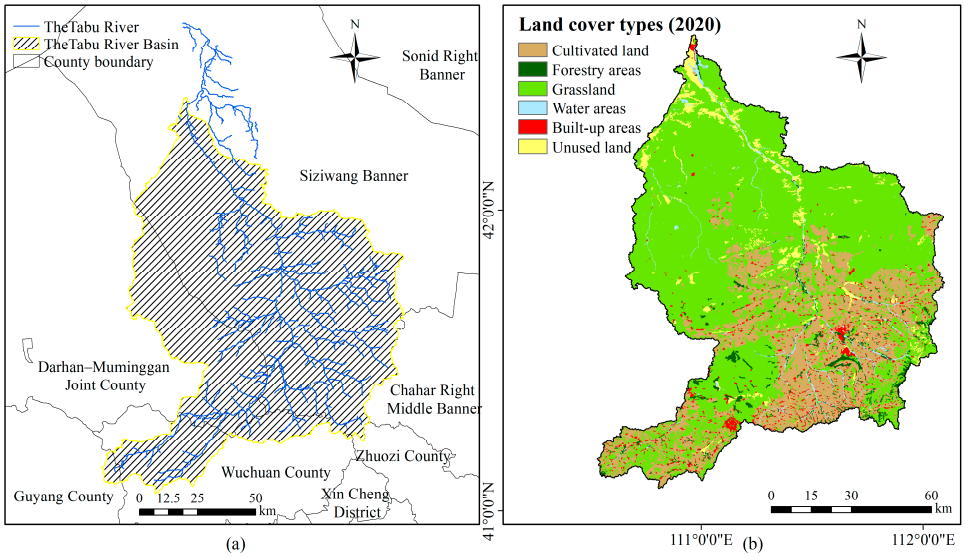


Figure 1. The geographical location of the entire Tabu River, showing the distribution of the mainstream and substream (**a**) and the study area of this research—the Tabu River Basin (**b**).

2.2. Data Sources

Datasets, including vector, raster, and statistical data, corresponding to the 2000 to 2020 period were used in this study (Table 1). All the vector and statistical data were rasterized and unified to a spatial resolution of 30 m × 30 m. Further, the Krasovsky_1940_Albers projection was used to unify the data to the coordinate system.

2.3. Evaluation of ESs

In this study, we quantitatively evaluated four pivotal ESs within the ecological context of the Tabu River Basin. These services included WY, HQ, FS, SF, and CS, which are affected by diverse land-use patterns (Table 2). Specific methodological steps are shown in the Supplementary Material.

Table 1. Data description.

Data Type	Data Source
Administrative boundaries	Resource and Environmental Science and Data Center (https://www.resdc.cn/, accessed on 1 January 2024)
Land cover—CNLUCC	Resource and Environmental Science and Data Center (https://www.resdc.cn/, accessed on 1 January 2024)
Meteorological data	National Tibetan Plateau/Third Pole Environment Data Center (https://data.tpdc.ac.cn/, accessed on 1 January 2024)
Soil texture	National Tibetan Plateau/Third Pole Environment Data Center (https://data.tpdc.ac.cn/, accessed on 1 January 2024)
DEM	Geospatial Data Cloud (https://www.gscloud.cn, accessed on 1 January 2024)
NDVI	MOD13Q1 NDVI data from NASA's Earth Data Center (https://search.earthdata.nasa.gov/, accessed on 1 January 2024)
Population data	Open Spatial Demographic Data and Research (https://www.worldpop.org/, accessed on 1 January 2024)

Table 2. Methodologies for quantifying ESs.

ESs	Methods	Formulars	
WY	InVEST [25].	$Y_{xj} = \left(1 - AET_{xj}/P_x\right) \times P_x$	(1)
HQ	InVEST [26].	$Q_{xj} = H_j\left(1 - \left(D_{xj}^Z/\left(D_{xj}^Z - k^z\right)\right)\right)$	(2)
FS	Empirical formulas [27].	$G_i = (NDVI_i/NDVI_{\text{sum}}) \times G_{\text{sum}}$	(3)
SF	Modified Revised Wind Erosion Equation (RWEQ) model [28,29].	$SP = SL_0 - SL_v$	(4)
		$SL(x) = Q_{max}\left\{1 - \exp\left[-(x/S)^2\right]\right\}$	(5)
		$Q_{max} = 109.8 \times WF \times EF \times K \times SCF \times C$	(6)
		$S = 150.71 \times (WF \times EF \times SCF \times K \times C)^{-0.3711}$	(7)
		$C = e^{-0.0438FVC}$	(8)
CS	Modified Carnegie Ames Stanford Approach (CASA) model [30].	$NPP(x,t) = ARAR(x,t) \times \varepsilon(x,t)$	(9)
		$ARAR(x,t) = 0.5 \times SOL(x,t) \times FRAR(x,t)$	(10)

2.4. Construction of an Ecological Security Pattern

2.4.1. Ecological Source Areas

Ecological source areas are patches that provide more ecological functions, play an essential role in the maintenance of ecosystem structure, and provide biological habitats [31]. The ecological core area was extracted using MSPA. Further, the high ES value area was extracted as the alternative ecological source area (Figure 2). Thereafter, the two were combined to obtain the integrated ecological source area (>10 km^2) [32].

2.4.2. Ecological Resistance Surface

Ecological resistance hinders processes such as the exchange of materials, the transfer of energy, and the migration of species between ecological sources and is influenced by natural conditions as well as human activities [33]. In this study, the resistance surface was constructed using land-use type, NDVI, population density, road distance, and elevation, with base resistance values standardized between 0 and 1 (Table 3). Based on the main hierarchical analysis and the actual situation in the study area, their weights were set to 0.26, 0.29, 0.11, 0.25, and 0.09 in order. As human activities intensify, natural habitats become increasingly fragmented, exacerbating biodiversity loss [34]. Further, landscape pattern indices, such as patch size, shape, and connectivity, can be used to assess habitat fragmentation and ecosystem degradation [35]. To adjust base resistance values, we incorporated the

largest patch index (LPI), aggregation index (AI), Shannon's diversity index (SHDI), and patch cohesion index (COHESION), all of which were determined using Fragstats 4.2 [35]. The specific equations used for determining these indices were obtained from a previous study [36]:

$$R_i = R \times F_{comi} \tag{11}$$

$$F_{comi} = a \cdot AI_{nor} + b \cdot COHESION_{nor} + c \cdot LPI_{nor} + d \cdot SHDI_{nor} \tag{12}$$

where, F_{comi} is the normalised landscape pattern composite index; R_i is the modified resistance coefficient; R is the value of the base resistance coefficient; AI_{nor}, $COHESION_{nor}$, LPI_{nor}, and $SHDI_{nor}$ are the values of the landscape pattern composite indices after normalisation, which were calculated using Fragstats 4.2 software; and a~d are the corresponding weights of the above four landscape pattern composite indices.

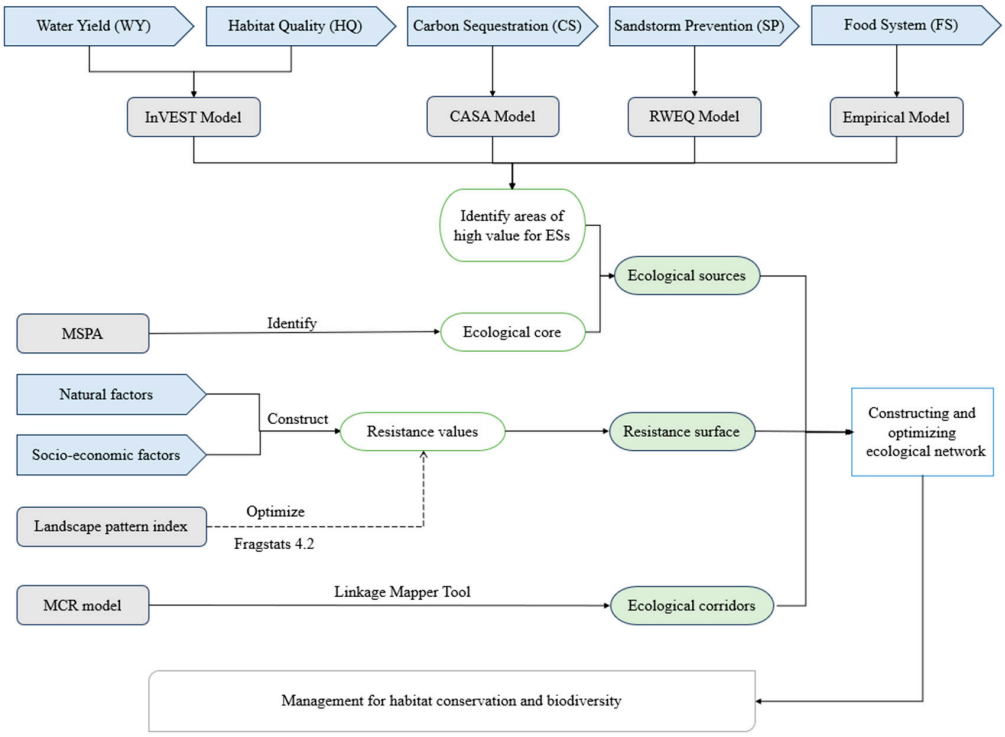


Figure 2. Research framework.

Table 3. Grading assignment and weight of resistance factor.

Resistance Factor	Grading Index		Resistance Value	Weight	Index Nature
Natural condition	Land-use type (LUCC)	Forestry areas/water areas	1	0.26	+
		Grassland	2		
		Cultivated land	3		
		Unused land	4		
		Build-up areas	5		
	NDVI		(0, 1)	0.29	–
Human interference	DEM		(0, 1)	0.11	+
	Road distance (RD)		(0, 1)	0.25	–
	Population density (PD)		(0, 1)	0.09	+

2.4.3. Ecological Corridor

Ecological corridors, which are pathways with low resistance values for ecological flow and exchange between different source patches, play an essential role in the flow of ecological substances [37], and can be divided into critical and potential corridors. Specifically, critical corridors are the least-cost pathways formed on the resistance surface between source patches, whereas potential corridors are the least-cost pathways that may be generated on the resistance surface between source patches [38]. Ecological pinch points refer to critical areas within an ecological network that lie in gaps or weak connections between ecological corridors, playing a vital role in enhancing ecological connectivity and facilitating species migration [39]. A Linkage Mapper tool [40] was used to identify ecological corridors in the landscape between the source and target sites.

3. Results

3.1. Spatiotemporal Pattern of ESs in the Tabu River Basin

From 2000 to 2020, all five ESs in the Tabu River Basin showed significant improvements (Figure 3). WY showed the greatest increase, whereas HQ, FS, and CS initially decreased, but later on showed an upward trend. Between 2000 and 2020, WY increased from 82 to 176 mm, FS increased from 451,000 to 763,000 t, and SF capacity increased from 4 to 31 t·km^{-2}. Further, CS fluctuated from 217 gC·m^{-2}·a^{-1} in 2000 and peaked at 265 gC·m^{-2}·a^{-1} in 2020. HQ also improved over time. It showed a slight decrease in 2010 but reached its highest value by 2020.

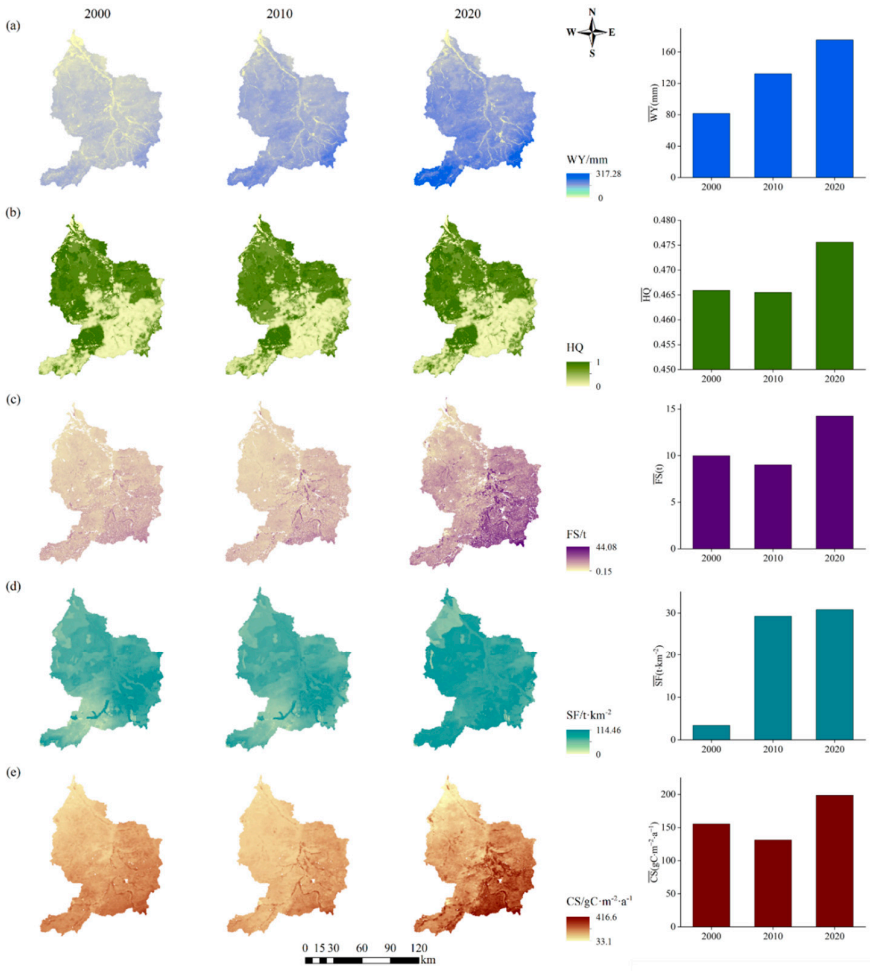


Figure 3. Spatiotemporal and annual average changes in ESs in the Tabu River Basin. (**a**) Water yield; (**b**) Habitat quality; (**c**) Food supply; (**d**) Sand fixation; (**e**) Carbon sequestration.

Spatially, WY and CS showed a pattern of higher values in the north and lower values in the south, whereas FS and SF showed higher values in the east and lower values in the west. Further, high-WY areas were concentrated in the southern mountainous forest regions, and the high-FS areas were primarily distributed in the southeastern part of the basin and gradually expanded westward. High-SF areas were located in the central and southeastern regions, predominantly in grasslands and croplands. By 2020, CS was higher in the south and lower in the north, with high-value areas expanding to the northwest. In contrast, HQ showed a pattern of higher values in the northwest and lower values in the southeast, mirroring the landscape structure. Specifically, the southern part of the basin demonstrated strong ES functions with respect to WY and CS, whereas the southeastern region played a key role with respect to FS and SF.

3.2. Landscape Pattern Indexes

3.2.1. Landscape Transformation

Within the 20-year study period, we observed increases in grassland area, followed by build-up areas and forestry areas, which increased by 186.21, 65.76, and 32.33 km^2, respectively, whereas arable land and unutilized land exhibited a significant decrease of 229.42 and 62.93 km^2, respectively (Figure 4). Additionally, three landscape types—unused land, grassland, and built-up areas—showed the largest conversion rates in the study area, at 15.56%, 9.60%, and 6.45%, respectively.

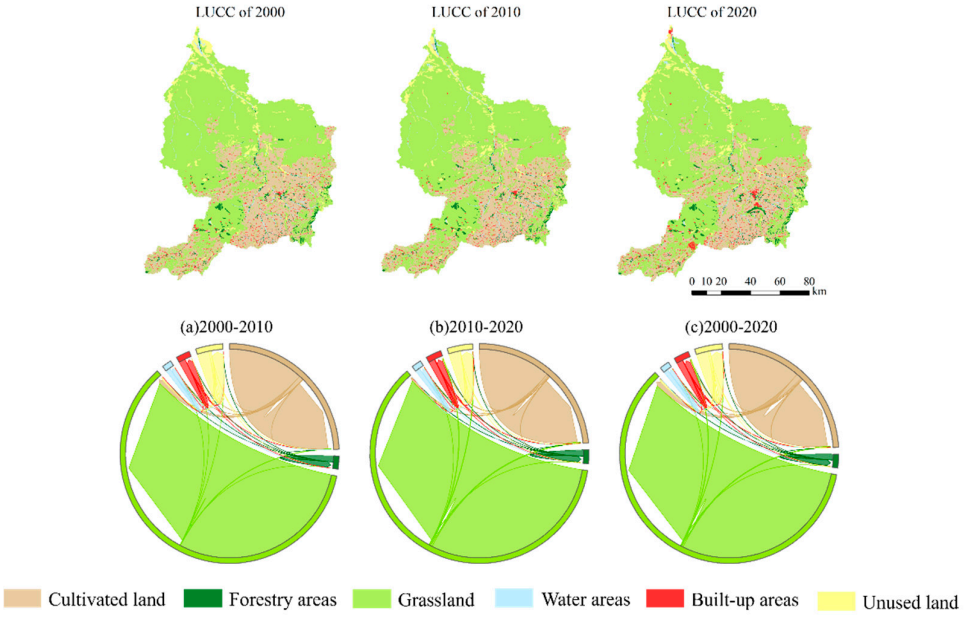


Figure 4. Landscape transformation in the Tabu River Basin between 2000 and 2020.

Within the study period, the transition from cultivated land to other land-use types changed significantly. Between 2000 and 2020, 2794.11 km^2 of cultivated land area remained unchanged, whereas 220.15 km^2 was converted to forest land and 7212.68 km^2 to grassland. Forest land also changed significantly, with 230.14 and 227.15 km^2 converted to grassland from 2000 to 2010 and from 2010 to 2020, respectively. Even though grassland largely remained unchanged, about 1.55% of the grassland has been converted into cultivated area, highlighting agricultural expansion. Further, unused land showed a significant transition to grassland (454.16 km^2). Overall, the Tabu River Basin has undergone dynamic land-use pattern changes, particularly between cultivated land, grassland, and forest land, reflecting an evolving landscape and shifts in ENs owing to human activities.

3.2.2. Changes in Landscape Pattern Indices

Overall, AI values for cropland, forest land, grassland, water, urban areas, and bare land showed minimal fluctuations over the 20-year study period (Table 4). Grassland consistently maintained a high AI (approximately 99), indicating good connectivity between grassland patches.

Table 4. Comparison of Landscape Pattern Indices in the Tabu River Basin between 2000 and 2020.

Landscape Pattern Index	2000						2020					
	Cropland	Forest	Grassland	Water	Urban	Bare	Cropland	Forest	Grassland	Water	Urban	Bare
AI	96.79	93.39	98.57	91.71	**92.17**	95.44	96.82	93.03	98.59	91.64	**91.44**	95.35
COHESION	99.77	97.12	99.94	98.78	**95.99**	98.38	99.86	96.89	99.93	98.80	**94.59**	98.24
DIVISION	0.99	1.00	0.77	1.00	1.00	1.00	0.99	1.00	0.76	1.00	1.00	1.00
LPI	**6.44**	0.14	47.69	0.17	**0.16**	0.26	**9.3870**	0.1023	47.81	0.17	**0.06**	0.21
LSI	**58.19**	36.82	**42.21**	37.89	**47.15**	34.04	**59.29**	36.97	**41.76**	37.76	**46.43**	34.06
PD	0.0514	**0.0295**	**0.0693**	0.0137	0.1011	0.0293	0.0503	**0.0487**	**0.6900**	0.0128	0.0950	0.0294
SPLIT	**156.65**	**162,405.88**	4.28	84,312.76	**170,104.93**	**35,838.22**	**94.99**	**246,972.26**	4.25	84,531.26	**901,114.46**	**46,033.97**
SHDI	**1.0059**						**0.9818**					

In contrast, the AI value for water bodies decreased slightly from 91.71 to 91.64. Additionally, grassland exhibited a consistently high COHESION value (approximately 99.94), indicative of strong spatial connectivity. However, the COHESION values for cropland and forest decreased slightly, with that of forests exhibiting a more notable decrease (from 97.12 to 96.89). Urban land exhibited a significant decline in connectivity. The DIVISION index for grassland decreased slightly from 0.77 to 0.76, indicating a lower level of fragmentation. Further, the fragmentation levels of cropland, forest, water, urban land, and bare land remained stable, indicating that there were no significant changes in landscape fragmentation over time. The LPI for grassland remained stable at approximately 48%, indicating its continued dominance in the landscape. Cropland LPI increased from 6.44 to 9.39, reflecting the expansion of cropland patches. In contrast, the LPI for urban land decreased, indicating that although urban areas expanded, they became more dispersed. Furthermore, the LSI for cropland increased slightly from 58.19 to 59.29, suggesting more complex shapes for the cropland patches. However, the grassland LSI decreased marginally, indicating more regular and possibly consolidated patch boundaries. The density of grassland patches remained stable, whereas cropland and forest PD indices decreased slightly, showing fewer patches, consistent with a trend towards landscape consolidation and land-use centralization. Grassland SPLIT decreased slightly, indicating improved connectivity among the patches. Conversely, cropland and urban land exhibited significant increases in SPLIT, reflecting a higher level of fragmentation. SHDI increased slightly over the 20-year period, indicating a more diverse land-cover pattern in the Tabu River Basin.

Between 2000 and 2020, the landscape pattern changes in the Tabu River Basin revealed shifts in land-use distribution. Within this period, both cropland and grassland expanded in terms of area and connectivity, with grassland maintaining dominance in the landscape. However, urban expansion intensified landscape fragmentation and reduced connectivity. These changes in the patterns of the landscape not only altered the structure and function of ENs, but may also impact the provision of ESs.

3.3. Ecological Security Patterns in the Tabu River Basin

3.3.1. Spatiotemporal Variations of ENs

In 2000, six ecological source patches, covering a total area of 1074.98 km^2, nine ecological corridors, spanning 394.29 km, and 27 ecological pinch points, primarily concentrated around source areas 3 and 5, were identified (Figure 5a). By 2020, the number of ecological source patches increased to 17, covering an area of 340.41 km^2, with 36 ecological corridors extending 756.76 km and 40 ecological pinch points distributed along the corridors (Figure 5b). Further, within the 20-year study period, the base resistance surface

in the northwestern and southeastern regions of the river basin significantly decreased and increased, respectively. This observation may be closely related to population growth in the southeastern region, where increasing development pressure intensifies ecological fragmentation. In contrast, the lower development intensity in the northwest led to a decrease in ecological resistance.

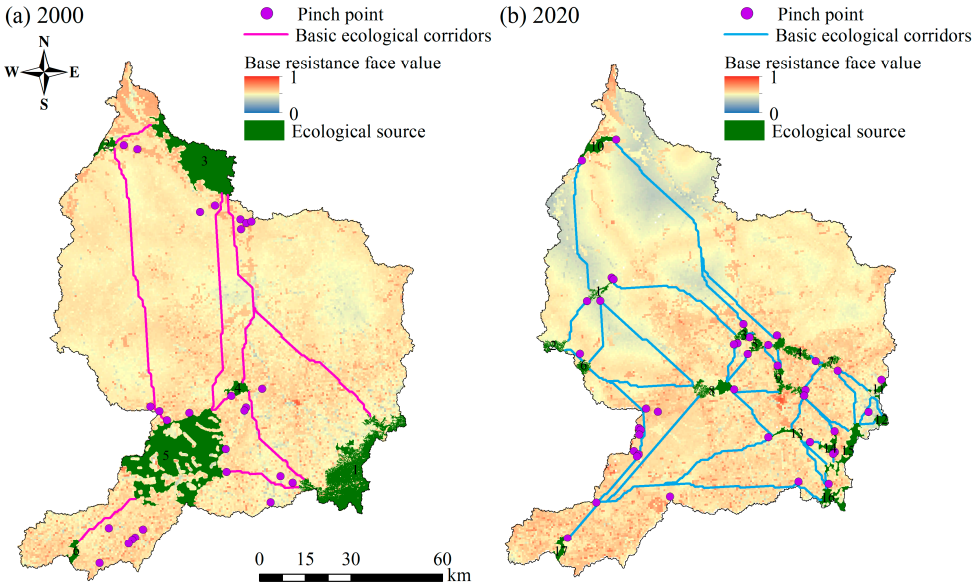


Figure 5. Comparison of ENs in the Tabu River Basin: 2000 vs. 2020.

Between 2000 and 2020, the ENs in the Tabu River Basin decreased by 13 ecological pinch points and 27 ecological corridors, but showed a total length decrease of 362.47 km (Figure 5). This observation suggests a decline in landscape connectivity over time in the study area. The decrease in the ecological pinch points indicates that fewer key areas contribute to biodiversity, whereas the decrease in corridor numbers and lengths implies reduced pathways for species movement and gene flow.

3.3.2. EN Optimization

In this study, we used the Linkage Mapper toolbox to generate ecological corridor distribution maps before and after resistance surface adjustments (Figure 6). The lengths of the ecological corridors were also determined. Thus, we observed significant changes in the ecological corridors in the Tabu River Basin. Before the adjustments, 36 ecological corridors, with a total length of 756.76 km were identified. After the adjustments, the number of ecological corridors increased to 37, with a total length of 869.97 km. Notably, new corridors were created between the 4th and 10th, 6th and 17th, and 7th and 14th ecological source areas, enhancing spatial continuity and connecting more ecological sources.

The number of ecological pinch points increased from 40 to 64, and growth was observed around each corridor. This observation indicates improved landscape connectivity and increased complexity and node connectivity within the ENs, enhancing system stability and resilience. Habitat fragmentation decreased with the optimized landscape pattern, showing a decrease in the number of isolated patches and improved species interactions and gene flow. These areas may serve as critical pathways for species migration and other ecological processes.

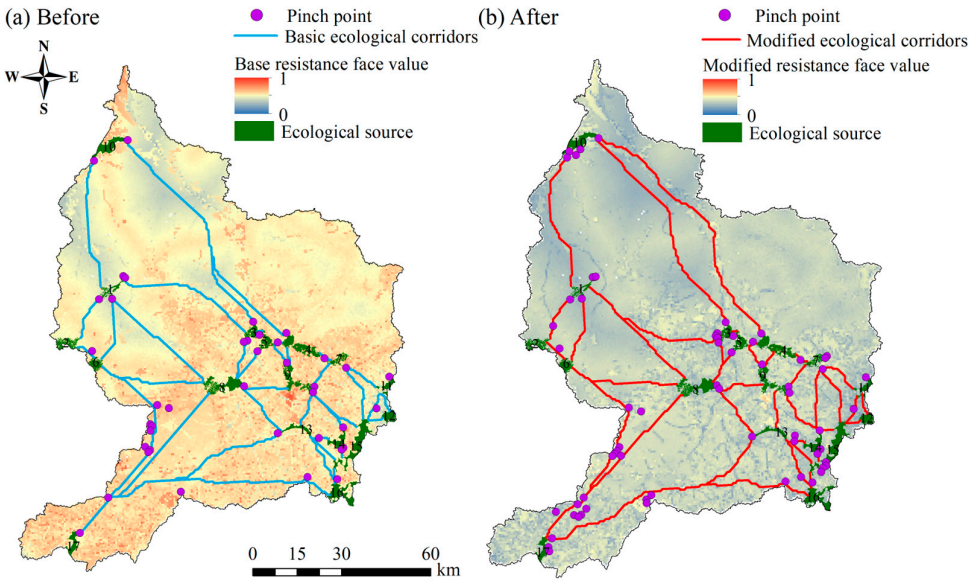


Figure 6. ENs in the Tabu River Basin before and after resistance surface correction.

After optimization, the overall resistance values decreased, showing a mean decrease of 0.18. Further, the most significant declines were observed in the northern and central-western regions of the basin. After optimizing biodiversity-related landscape pattern indices, the overall resistance values decreased and the spatial distribution of resistance strength remained consistent. This finding indicated that although the landscape structure improved and the overall ecological functionality was enhanced during the optimization process, regional differences in resistance did not change significantly.

From a network connectivity perspective (Table 5), both the original resistance surface and the resistance surface modified based on landscape pattern indices formed relatively closed EN structures in space. Further, relative to the original resistance surface, the spatial structure of the ENs, based on the modified resistance surface, showed a higher degree of closure. The α index increased by 0.14, indicating a higher level of connectivity of ecological corridors within the region and facilitating smoother species migration. The β index increased by 0.44, suggesting a more complex network structure. The β index was > 1, confirming a reticular network structure. Additionally, the γ index increased by 0.10, indicating an improvement in node connectivity.

Table 5. EN structure indices before and after resistance surface correction.

Index	Before	After
β	2.92	3.36
α	0.27	0.41
γ	0.52	0.62

4. Discussion

4.1. Building ENs Based on ESs

To date, studies on the construction of ENs have primarily employed MSPA [41], whereas studies on the role of ESs and landscape pattern indices in the analysis and optimization of these networks are limited [42]. The spatial modeling of ecosystem services is fundamental for identifying landscape elements, and the accuracy and reliability of these modeling processes are crucial for establishing effective ecological security patterns [43].

In this study, we have shown that the use of ESs for the identification of ecological source areas and for the establishment of ENs is an effective strategy for enhancing landscape connectivity (Table 6). Key ESs, such as WY, SF, and CS, are vital for identifying areas of ecological significance [44]. By spatially overlapping these services, priority

zones for conservation can be highlighted, aligning well with the goal of maintaining ecological balance [45]. Further, incorporating the flow of ecosystem services into corridor design enhances the functionality of ENs, improving species migration and resource distribution [15].

Table 6. The dPC and dIIC of ecological sources.

Sort Number	Node	Shape Area	dIIC	dPC
1	15	42.62	34.99	33.63
2	4	32.74	25.68	24.26
3	16	29.28	17.96	16.61
4	9	27.16	14.72	16.17
5	5	14.94	12.00	14.18
6	8	37.64	9.07	13.56
7	14	15.59	9.11	12.04
8	7	11.86	6.04	8.74
9	3	13.74	6.16	8.65
10	12	12.47	10.97	7.62
11	13	12.48	1.00	6.77
12	11	10.32	4.87	4.91
13	10	25.64	4.21	3.01
14	2	14.88	2.65	2.17
15	6	12.89	2.29	1.84
16	1	11.86	0.90	1.00
17	17	14.30	1.31	0.93

4.2. Landscape Pattern Indices and Resistance Surfaces

Land-use transfer matrix analysis using 2000–2020 data revealed significant land-use shifts in the Tabu River Basin, particularly with respect to transitions between cultivated land, grassland, and forest land. The conversion of grassland to cultivated land indicated growing agricultural pressure and highlighted increasing demand for natural resources [42,46]. These changes altered landscape pattern indices and affected ENs, consistent with previously reported findings [47]. Forest land and unused land were converted to cultivated land and built-up areas, indicating intensifying land use and urbanization [48]. Although some grassland areas showed resilience, the overall trend underscored the need for sustainable land management to balance development with ecological conservation and the preservation of biodiversity and ecosystem functions [49,50].

The observed decline in ENs during the study period, accompanied by a decrease in the number of ecological nodes, corridors, and overall connectivity, suggested weakening of the region's ecological integrity [51]. Reportedly, the loss of ecological nodes and corridors indicated dependence on fewer critical areas as support for biodiversity. Our results also included diminished pathways for species movement and gene flow [52]. This fragmentation was exacerbated by increased resistance in the southeastern region, driven by population growth and development-related pressures [53]. Conversely, the northwest, with a lower level of development intensity, showed a decrease in resistance, indicative of a relatively stable ecological environment [54].

Resistance surface optimization using landscape pattern indices significantly improved EN connectivity and model effectiveness. Specifically, by refining the resistance surface using indices, such as AI, COHESION, LPI, and SHDI, the model better reflected the impact of landscape use patterns on species movement. This optimization increased the number of ecological corridors, extended their total length, enhanced species migration pathways, and promoted biodiversity [55]. Grasslands, identified as high-function areas, showed a greater level of ecological node connection post-optimization, aligning with the determined landscape indices [56]. Although the number of ecological nodes decreased, there was an overall improvement in the complexity and robustness of the network, enhancing ecosystem functionality [57].

In summary, the Tabu River Basin has experienced dynamic land-use changes as well as a decline in ecological connectivity over the past 20 years. These trends highlight the need for balanced land-use management strategies for mitigating the negative impacts of development while preserving key ecological functions and maintaining landscape connectivity [58]. The optimization of the resistance surface also served as a scientific basis for targeted ecological restoration and can support future conservation and planning efforts to enhance the region's ecological resilience [59,60].

4.3. Management Measures Based on ENs and ESs

Based on ESs and ENs, we delineated four types of ecological management zones (Figure 7). The first, which was the core ecological protection zone, located primarily in the southeastern and southwestern regions of the basin, constituted areas with high ES values and critical ecological node overlap [61]. These zones were designated for ecological protection and restoration and required strict limitations on development [62]. Second, we delineated the ecological corridor zone, predominantly located in the southwestern part of the basin and connecting the core areas, with a higher number of ecological pinch points and requiring careful management to maintain species migration pathways and minimize human disturbance [63]. The third zone was the ecological restoration zone, situated in the northern part of the basin. It is characterized by a low ES but has high potential for improvement [64]. Ecological restoration efforts should focus on this zone to enhance its function [65]. Finally, we identified the ecological utilization zone, located in the western region and characterized by moderate ES levels [66]. The areas in this zone could be sustainably utilized for agriculture, forestry, or ecotourism, provided that they do not disrupt the connectivity of the ENs or compromise the protection of core ecological zones [67].

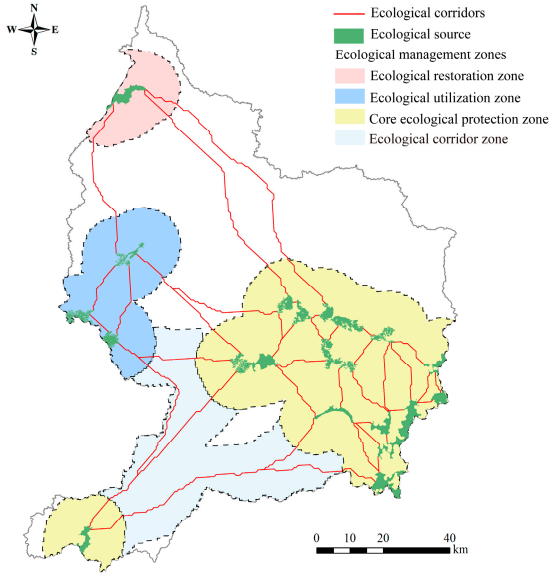


Figure 7. Zoning of the Tabu River Basin for Ecological management.

5. Conclusions

In this study, we integrated ESs with the MSPA model to identify ecological sources and used landscape pattern indices to optimize the resistance surface. Finally, we constructed ENs using the MCR model. The main conclusions are as follows:

From 2000 to 2020, the five typical ESs in the Tabu River Basin, namely, WY, HQ, FS, SF, and CS, increased, with 70% of the southeast region showing an increase in ESs. Further, within the study period, landscape pattern indices changed considerably owing to the conversion of cultivated land, grassland, and unused land to other land types. The number of ecological source areas increased; however, their total area decreased,

leading to heightened landscape fragmentation. Further, after optimization, the number of ecological corridors and ecological pinch points increased. The β, α, and γ indices also improved. Thus, we proposed spatial management strategies based on the optimized ENs for biodiversity conservation.

Frequent human activities have led to biodiversity loss and increased landscape fragmentation. To tackle this challenge moving forward, it will be necessary to carefully construct ENs. This study offers important insights for optimizing ecological conservation and land-use planning. Based on the results obtained, the implementation of vegetation restoration and soil conservation measures to enhance ESs are highly recommended. Additionally, areas with high ecological value should be strictly protected to strengthen ecological security. Finally, optimizing corridor design may support habitat preservation and species migration, thereby promoting biodiversity conservation.

Supplementary Materials: The following supporting information can be downloaded at: https://www.mdpi.com/article/10.3390/land13122209/s1.

Author Contributions: Conceptualization, methodology, software, formal analysis, data curation, and writing—original draft, W.Z.; writing—review and editing and visualization, Y.F.; writing—review and editing, visualization, supervision, project administration, and funding acquisition, B.W. All authors have read and agreed to the published version of the manuscript.

Funding: This research was supported and funded by the Key Project of the Collaborative Innovation Center for Grassland Ecological Security (YSZD202301) and the National Natural Science Foundation of China (32060316).

Data Availability Statement: Data are available upon request due to restrictions. The data presented in this study are available upon request from the corresponding author. The data are not publicly available to protect privacy and anonymity.

Conflicts of Interest: The authors declare that they have no known competing financial interests or personal relationships that could have appeared to influence the work reported in this paper.

References

1. Sadat Nickayin, S.; Egidi, G.; Cudlin, P.; Salvati, L. Investigating metropolitan change through mathematical morphology and a dynamic factor analysis of structural and functional land-use indicators. *Sci. Rep.* **2023**, *13*, 695. [CrossRef]
2. Sidemo-Holm, W.; Ekroos, J.; Reina García, S.; Söderström, B.; Hedblom, M. Urbanization causes biotic homogenization of woodland bird communities at multiple spatial scales. *Glob. Change Biol.* **2022**, *28*, 6152–6164. [CrossRef]
3. Ding, G.; Yi, D.; Yi, J.; Jie, G.; OU, M.; Ou, W.; Yu, T.; Pueppke, S.G. Protecting and Constructing Ecological Corridors for Biodiversity Conservation: A Framework That Integrates Landscape Similarity Assessment. *Appl. Geogr.* **2023**, *160*, 103098. [CrossRef]
4. Justeau-Allaire, D.; Ibanez, T.; Vieilledent, G.; Lorca, X.; Birnbaum, P. Refining intra-patch connectivity measures in landscape fragmentation and connectivity indices. *Landsc. Ecol.* **2024**, *39*, 24. [CrossRef]
5. Keyes, A.A.; McLaughlin, J.P.; Barner, A.K.; Dee, L.E. An ecological network approach to predict ecosystem service vulnerability to species losses. *Nat. Commun.* **2021**, *12*, 1586. [CrossRef]
6. Lu, Z.; Geng, Y.; Li, W.; Yue, R. Integrating spatial carbon factors into ecological network construction in an energy-intensive megaregion toward multi-objective synergy in northern China. *Environ. Impact Assess. Rev.* **2024**, *106*, 107480. [CrossRef]
7. Daily, G.C. Nature's Services: Societal Dependence on Natural Ecosystems (1997). *Future Nat.* **2017**, *41*, 454–464. [CrossRef]
8. Millennium Ecosystem Assessment. *Millennium Ecosystem Assessment Ecosystems and Human Well-Being*; Island Press: Washington, DC, USA, 2005; ISBN 9781597260428.
9. Costanza, R.; d'Arge, R.; de Groot, R.; Farber, S.; Grasso, M.; Hannon, B.; Limburg, K.; Naeem, S.; O'Neill, R.V.; Paruelo, J.; et al. The Value of the World's Ecosystem Services and Natural Capital. *Ecol. Econ.* **1998**, *25*, 3–15. [CrossRef]
10. Jia, Q.; Jiao, L.; Lian, X.; Wang, W. Linking Supply-Demand Balance of Ecosystem Services to Identify Ecological Security Patterns in Urban Agglomerations. *Sustain. Cities Soc.* **2023**, *92*, 104497. [CrossRef]
11. Modica, G.; Praticò, S.; Laudari, L.; Ledda, A.; Di Fazio, S.; De Montis, A. Implementation of multispecies ecological networks at the regional scale: Analysis and multi-temporal assessment. *J. Environ. Manag.* **2021**, *289*, 112494. [CrossRef]
12. Qin, J.; Dai, J.; Li, S.; Zhang, J.; Peng, J. Construction of Ecological Network in Qujing City Based on MSPA and MCR Models. *Sci. Rep.* **2024**, *14*, 9800. [CrossRef]
13. Lu, Y.; Huang, D.; Tong, Z.; Liu, Y.; He, J.; Liu, Y. A conceptual framework for constructing and evaluating directed ecological networks: Evidence from Wuhan Metropolitan Area, China. *Environ. Impact Assess. Rev.* **2024**, *106*, 107464. [CrossRef]

14. Xu, A.; Hu, M.; Shi, J.; Bai, Q.; Li, X. Construction and optimization of ecological network in inland river basin based on circuit theory, complex network and ecological sensitivity: A case study of Gansu section of Heihe River Basin. *Ecol. Model.* **2024**, *488*, 110578. [CrossRef]
15. Yang, Y.; Wang, Z.; Li, B.; Guan, J. The Impact of Photovoltaic Projects on Ecological Corridors through the Least-Cost Path Model. *Glob. Ecol. Conserv.* **2023**, *42*, e02381. [CrossRef]
16. Huang, H.; Fu, D.; Ding, G.; Yan, C.; Xie, X.; Gao, Y.; Liu, Q. Construction and Optimization of Green Infrastructure Network in Mountainous Cities: A Case Study of Fuzhou, China. *Sci. Rep.* **2024**, *14*, 11936. [CrossRef]
17. Peng, J.; Zhao, S.; Dong, J.; Liu, Y.; Meersmans, J.; Li, H.; Wu, J. Applying Ant Colony Algorithm to Identify Ecological Security Patterns in Megacities. *Environ. Model. Softw.* **2019**, *117*, 214–222. [CrossRef]
18. Zhou, X.; Chu, Z.; Ji, X. Changes in the Landuse Landscape Pattern and Ecological Network of Xuzhou Planning Area. *Sci. Rep.* **2024**, *14*, 8854. [CrossRef]
19. Miliša, M.; Stubbington, R.; Datry, T.; Cid, N.; Bonada, N.; Šumanović, M.; Milošević, D. Taxon-Specific Sensitivities to Flow Intermittence Reveal Macroinvertebrates as Potential Bioindicators of Intermittent Rivers and Streams. *Sci. Total Environ.* **2022**, *804*, 150022. [CrossRef]
20. Cottet, M.; Robert, A.; Tronchère-Cottet, H.; Datry, T. "It's Dry, It Has Fewer Charms!": Do Perceptions and Values of Intermittent Rivers Interact with Their Management? *Environ. Sci. Policy* **2023**, *139*, 139–148. [CrossRef]
21. Acuña, V.; Datry, T.; Marshall, J.; Barceló, D.; Dahm, C.N.; Ginebreda, A.; McGregor, G.; Sabater, S.; Tockner, K.; Palmer, M.A. Why Should We Care about Temporary Waterways? *Science* **2014**, *343*, 1080–1081. [CrossRef]
22. Fortesa, J.; Ricci, G.F.; García-Comendador, J.; Gentile, F.; Estrany, J.; Sauquet, E.; Datry, T.; De Girolamo, A.M. Analysing Hydrological and Sediment Transport Regime in Two Mediterranean Intermittent Rivers. *Catena* **2021**, *196*, 104865. [CrossRef]
23. Wu, L.; Luo, Y.; Pang, S.; Wang, G.; Ma, X. Factor Analysis of Hydrologic Services in Water-Controlled Grassland Ecosystems by InVEST Model and Geodetector. *Environ. Sci. Pollut. Res.* **2024**, *31*, 20409–20433. [CrossRef] [PubMed]
24. Luo, J.; Yu, R.; Liang, W.; Hao, Y. Scale-specific controls of monthly suspended sediment load in a typical inland river. *J. Hydrol.* **2024**, *641*, 131847. [CrossRef]
25. Wang, X.; Wang, B.; Cui, F. Exploring ecosystem services interactions in the dryland: Socio-ecological drivers and thresholds for better ecosystem management. *Ecol. Indic.* **2024**, *159*, 111699. [CrossRef]
26. Xu, Z.; Peng, J.; Liu, Y.; Qiu, S.; Zhang, H.; Dong, J. Exploring the combined impact of ecosystem services and urbanization on SDGs realization. *Appl. Geogr.* **2023**, *153*, 102907. [CrossRef]
27. Ouyang, X.; Tang, L.; Wei, X.; Li, Y. Spatial Interaction between Urbanization and Ecosystem Services in Chinese Urban Agglomerations. *Land Use Policy* **2021**, *109*, 105587. [CrossRef]
28. Fryrear, W.; Saleh, N.A.; Bilbro, D. A SINGLE EVENTWIND EROSION MODEL. *Trans. ASAE* **1998**, *41*, 1369–1374. [CrossRef]
29. Zhu, W.; Zhang, Z.; Zhang, H.; Tovuudorj, R. Integrating Spatial Patterns and Driving Factors of Cultural Ecosystem Services into Territorial Spatial Governance: A Case Study of the Horqin Sandy Land with Multi-Ethnic Settlements. *Habitat Int.* **2024**, *148*, 103093. [CrossRef]
30. Zhu, W.; Pan, Y.; He, H.; Yu, D.; Hu, H. Simulation of Maximum Light Use Efficiency for Some Typical Vegetation Types in China. *Chin. Sci. Bull.* **2006**, *51*, 457–463. [CrossRef]
31. Peng, J.; Yang, Y.; Liu, Y.; Hu, Y.; Du, Y.; Meersmans, J.; Qiu, S. Linking Ecosystem Services and Circuit Theory to Identify Ecological Security Patterns. *Sci. Total Environ.* **2018**, *644*, 781–790. [CrossRef]
32. Saura, S.; Bodin, Ö.; Fortin, M.-J. Stepping Stones Are Crucial for Species' Long-Distance Dispersal and Range Expansion through Habitat Networks. *J. Appl. Ecol.* **2013**, *51*, 171–182. [CrossRef]
33. Betts, M.G.; Wolf, C.; Ripple, W.J.; Phalan, B.; Millers, K.A.; Duarte, A.; Butchart, S.H.M.; Levi, T. Global Forest Loss Disproportionately Erodes Biodiversity in Intact Landscapes. *Nature* **2017**, *547*, 441–444. [CrossRef]
34. Babí Almenar, J.; Bolowich, A.; Elliot, T.; Geneletti, D.; Sonnemann, G.; Rugani, B. Assessing Habitat Loss, Fragmentation and Ecological Connectivity in Luxembourg to Support Spatial Planning. *Landsc. Urban Plan.* **2019**, *189*, 335–351. [CrossRef]
35. McGarigal, K.; Cushman, S.A.; Neel, M.C.; Ene, E. *FRAGSTATS v4: Spatial Pattern Analysis Program for Categorical Maps*; University of Massachusetts: Amherst, MA, USA, 2023.
36. Shen, R.; Shi, Z.; He, G.; Lin, Y.; Xu, R. Construction and Optimization of the Ecological Security Pattern of Xishuangbanna Based on Fragmentation Index. *Trop. Geogr.* **2022**, *42*, 1363–1375. [CrossRef]
37. Liu, H.; Wang, Z.; Zhang, L.; Tang, F.; Wang, G.; Li, M. Construction of an Ecological Security Network in the Fenhe River Basin and Its Temporal and Spatial Evolution Characteristics. *J. Clean. Prod.* **2023**, *417*, 137961. [CrossRef]
38. Salviano, I.R.; Gardon, F.R.; dos Santos, R.F. Ecological Corridors and Landscape Planning: A Model to Select Priority Areas for Connectivity Maintenance. *Landsc. Ecol.* **2021**, *36*, 3311–3328. [CrossRef]
39. Beier, P.; Noss, R.F. Do Habitat Corridors Provide Connectivity? *Conserv. Biol.* **1998**, *12*, 1241–1252. [CrossRef]
40. McRae, B.H.; Hall, S.A.; Beier, P.; Theobald, D.M. Where to Restore Ecological Connectivity? Detecting Barriers and Quantifying Restoration Benefits. *PLoS ONE* **2012**, *7*, e52604. [CrossRef]
41. Ma, T.Z.; The, B.T.; Kho, M.Y. Land Use Change and Ecological Network in Rapid Urban Growth Region in Selangor Region, Malaysia. *Sci. Rep.* **2024**, *14*, 16470. [CrossRef]
42. An, Y.; Liu, S.; Sun, Y.; Shi, F.; Beazley, R. Construction and Optimization of an Ecological Network Based on Morphological Spatial Pattern Analysis and Circuit Theory. *Landsc. Ecol.* **2020**, *36*, 2059–2076. [CrossRef]

43. Wang, K.; Zhang, C.; Chen, H.; Yue, Y.; Zhang, W.; Zhang, M.; Qi, X.; Fu, Z. Karst Landscapes of China: Patterns, Ecosystem Processes and Services. *Landsc. Ecol.* **2019**, *34*, 2743–2763. [CrossRef]
44. Wang, X.; Sun, Z.; Feng, X.; Ma, J.; Jia, Z.; Wang, X.; Zhou, J.; Zhang, X.; Yao, W.; Tu, Y. Identification of Priority Protected Areas in Yellow River Basin and Detection of Key Factors for Its Optimal Management Based on Multi-Scenario Trade-off of Ecosystem Services. *Ecol. Eng.* **2023**, *194*, 107037. [CrossRef]
45. Mitchell, M.G.E.; Schuster, R.; Jacob, A.L.; Hanna, D.E.L.; Dallaire, C.O.; Raudsepp-Hearne, C.; Bennett, E.M.; Lehner, B.; Chan, K.M.A. Identifying Key Ecosystem Service Providing Areas to Inform National-Scale Conservation Planning. *Environ. Res. Lett.* **2021**, *16*, 014038. [CrossRef]
46. Wolff, S.; Schrammeijer, E.A.; Schulp, C.J.E.; Verburg, P.H. Meeting Global Land Restoration and Protection Targets: What Would the World Look like in 2050? *Glob. Environ. Change* **2018**, *52*, 259–272. [CrossRef]
47. Sangermano, F. Acoustic Diversity of Forested Landscapes: Relationships to Habitat Structure and Anthropogenic Pressure. *Landsc. Urban Plan.* **2022**, *226*, 104508. [CrossRef]
48. Martins, I.S.; Dornelas, M.; Vellend, M.; Thomas, C.D. A Millennium of Increasing Diversity of Ecosystems until the Mid-20th Century. *Glob. Change Biol.* **2022**, *28*, 5945–5955. [CrossRef]
49. Dang, H.; Lü, Y.; Wang, X.; Hao, Y.; Fu, B. Integrating Species Diversity, Ecosystem Services, Climate and Ecological Stability Helps to Improve Spatial Representation of Protected Areas for Quadruple Win. *Geogr. Sustain.* **2024**, *In Press*. [CrossRef]
50. Shipley, J.R.; Frei, E.R.; Bergamini, A.; Boch, S.; Schulz, T.; Ginzler, C.; Barandun, M.; Bebi, P.; Bolliger, J.; Bollmann, K.; et al. Agricultural Practices and Biodiversity: Conservation Policies for Semi-Natural Grasslands in Europe. *Curr. Biol.* **2024**, *34*, R753–R761. [CrossRef]
51. Luo, Y.; Wu, J. Linking the Minimum Spanning Tree and Edge Betweenness to Understand Arterial Corridors in an Ecological Network. *Landsc. Ecol.* **2021**, *36*, 1549–1565. [CrossRef]
52. Gao, J.; Gong, J.; Li, Y.; Yang, J.; Liang, X. Ecological Network Assessment in Dynamic Landscapes: Multi-Scenario Simulation and Conservation Priority Analysis. *Land Use Policy* **2024**, *139*, 107059. [CrossRef]
53. Haddad, N.M.; Brudvig, L.A.; Clobert, J.; Davies, K.F.; Gonzalez, A.; Holt, R.D.; Lovejoy, T.E.; Sexton, J.O.; Austin, M.P.; Collins, C.D.; et al. Habitat Fragmentation and Its Lasting Impact on Earth's Ecosystems. *Sci. Adv.* **2015**, *1*, e1500052. [CrossRef] [PubMed]
54. Zhang, T.; Ji, X.; Xu, M.; Zhao, G.; Zheng, Z.; Tang, Y.; Chen, N.; Zhu, J.; He, Y.; Zhang, Y. Influences of Drought on the Stability of an Alpine Meadow Ecosystem. *Ecosyst. Health Sustain.* **2022**, *8*, 2110523. [CrossRef]
55. Kang, J.; Zhang, X.; Zhu, X.; Zhang, B. Ecological Security Pattern: A New Idea for Balancing Regional Development and Ecological Protection. A Case Study of the Jiaodong Peninsula, China. *Glob. Ecol. Conserv.* **2021**, *26*, e01472. [CrossRef]
56. Zhao, Q.; Yu, K.; Geng, J.; Lin, J.; Ai, J.; Liu, J. Spatiotemporal Evolution of Urban Heat Islands and Optimization of Spatial Network Construction in the Central Urban Area of Fuzhou City, China. *Chin. Geogr. Sci.* **2024**, *34*, 917–930. [CrossRef]
57. Yuan, M.M.; Guo, X.; Wu, L.; Zhang, Y.; Xiao, N.; Ning, D.; Shi, Z.; Zhou, X.; Wu, L.; Yang, Y.; et al. Climate Warming Enhances Microbial Network Complexity and Stability. *Nat. Clim. Change* **2021**, *11*, 343–348. [CrossRef]
58. Estrada-Carmona, N.; Hart, A.K.; DeClerck, F.A.J.; Harvey, C.A.; Milder, J.C. Integrated Landscape Management for Agriculture, Rural Livelihoods, and Ecosystem Conservation: An Assessment of Experience from Latin America and the Caribbean. *Landsc. Urban Plan.* **2014**, *129*, 1–11. [CrossRef]
59. Xu, D.; Peng, J.; Jiang, H.; Dong, J.; Liu, M.; Chen, Y.; Wu, J.; Meersmans, J. Incorporating Barriers Restoration and Stepping Stones Establishment to Enhance the Connectivity of Watershed Ecological Security Patterns. *Appl. Geogr.* **2024**, *170*, 103347. [CrossRef]
60. Kim, J.; Song, Y. Integrating Ecosystem Services and Ecological Connectivity to Prioritize Spatial Conservation on Jeju Island, South Korea. *Landsc. Urban Plan.* **2023**, *239*, 104865. [CrossRef]
61. Zhou, Q.; van den Bosch, C.C.K.; Chen, J.; Zhang, W.; Dong, J. Identification of Ecological Networks and Nodes in Fujian Province Based on Green and Blue Corridors. *Sci. Rep.* **2021**, *11*, 20872. [CrossRef]
62. Xu, W.; Li, X.; Pimm, S.L.; Hull, V.; Zhang, J.; Zhang, L.; Xiao, Y.; Zheng, H.; Ouyang, Z. The Effectiveness of the Zoning of China's Protected Areas. *Biol. Conserv.* **2016**, *204*, 231–236. [CrossRef]
63. Poor, E.E.; Scheick, B.; Cox, J.J.; Guthrie, J.M.; Mullinax, J.M. Towards Robust Corridors: A Validation Framework to Improve Corridor Modeling. *Landsc. Ecol.* **2024**, *39*, 177. [CrossRef]
64. Li, R.; Zheng, H.; O'Connor, P.; Xu, H.; Li, Y.; Lu, F.; Robinson, B.E.; Ouyang, Z.; Hai, Y.; Daily, G.C. Time and Space Catch up with Restoration Programs That Ignore Ecosystem Service Trade-Offs. *Sci. Adv.* **2021**, *7*, eabf8650. [CrossRef] [PubMed]
65. Pedrini, S.; Dixon, K.W. International Principles and Standards for Native Seeds in Ecological Restoration. *Restor. Ecol.* **2020**, *24*, S286–S303. [CrossRef]
66. Hu, Y.; Gong, J.; Li, X.; Song, L.; Zhang, Z.; Zhang, S.; Zhang, W.; Dong, J.; Dong, X. Ecological Security Assessment and Ecological Management Zoning Based on Ecosystem Services in the West Liao River Basin. *Ecol. Eng.* **2023**, *192*, 106973. [CrossRef]
67. Mathevet, R.; Thompson, J.D.; Folke, C.; Chapin, F.S. Protected Areas and Their Surrounding Territory: Socioecological Systems in the Context of Ecological Solidarity. *Ecol. Appl.* **2016**, *26*, 5–16. [CrossRef]

Disclaimer/Publisher's Note: The statements, opinions and data contained in all publications are solely those of the individual author(s) and contributor(s) and not of MDPI and/or the editor(s). MDPI and/or the editor(s) disclaim responsibility for any injury to people or property resulting from any ideas, methods, instructions or products referred to in the content.